

Inhibition of Amiloride-sensitive Apical Na^+ Conductance by Acetylcholine in Rabbit Cortical Collecting Duct Perfused In Vitro

Masahiro Takeda, Koji Yoshitomi, Junichi Taniguchi, and Masashi Imai

Department of Pharmacology, Jichi Medical School, Tochigi 329-04, Japan

Abstract

We examined effects of acetylcholine (ACh) on the electrical parameters and intracellular Ca^{2+} concentration ($[\text{Ca}^{2+}]_i$) in the isolated rabbit cortical collecting duct (CCD) perfused in vitro using the conventional microelectrode technique and microscopic fluorescence spectrophotometry. ACh (10^{-8} to 10^{-5} M) in the bath caused a positive deflection of the transepithelial voltage (V_T) and an increase in $[\text{Ca}^{2+}]_i$. Carbachol also showed similar but smaller effects. The effects of ACh were antagonized by muscarinic receptor antagonists. ACh at 10^{-6} M hyperpolarized the apical membrane voltage and increased the fractional resistance of the apical membrane of the collecting duct cells accompanied by a positive deflection of V_T and an increase in transepithelial resistance, whereas it did not affect these parameters in the β -intercalated cells. In the presence of 10^{-5} M amiloride in the lumen, the effects of ACh were almost completely abolished. The ACh-induced increase in $[\text{Ca}^{2+}]_i$ is accounted for by the release of Ca^{2+} from intracellular store and Ca^{2+} entry from the bath. In the absence of Ca^{2+} in the bath, the ACh-induced changes in electrophysiological parameters were significantly smaller than those observed in the presence of Ca^{2+} . Both phorbol-12-myristate-13-acetate (PMA) and phorbol-12,13-dibutyrate (PDBu), activators of protein kinase C (PKC), also inhibited the apical Na^+ conductance. In the presence of PMA or PDBu in the bath, ACh did not show further inhibitory effect. 1-(5-Isoquinolinylylsulfonyl)-2-methylpiperazine, an inhibitor of PKC, partially attenuated the effect of ACh. These observations indicate that ACh inhibits the apical Na^+ conductance partly by both increasing $[\text{Ca}^{2+}]_i$ and activating PKC. Such an action of ACh may partially explain its natriuretic effect. (J. Clin. Invest. 1994; 93:2649-2657.)

Key words: acetylcholine • Na^+ transport • cortical collecting duct • intracellular Ca^{2+} • protein kinase C

Introduction

Infusion of acetylcholine (ACh)¹ into the renal artery has been demonstrated to increase urinary excretion of water and Na^+ .

Address correspondence to Dr. Masashi Imai, Department of Pharmacology, Jichi Medical School, Minamikawachi, Kawachi, Tochigi 329-04, Japan.

Received for publication 29 November 1993 and in revised form 1 February 1994.

1. Abbreviations used in this paper: ACh, acetyl choline; CCh, carbachol; CCD, cortical collecting duct; CD cell, collecting duct cell; fR_A, fractional apical membrane resistance; H-7, 1-(5-isoquinolinylylsulfonyl)-2-methylpiperazine; IC cell, intercalated cell; PDBu,

Although such maneuver consistently increased renal plasma flow and decreased renal arteriolar resistance, it caused variable or no changes in GFR (1, 2). Therefore, this phenomenon has been thought to be ascribed not only to changes in renal hemodynamics but also to an inhibition of the tubular Na^+ reabsorption.

Recently, several lines of evidence have accumulated in support of the view that the kidney is innervated by parasympathetic nerves and that ACh receptors exist in the nephrons. Pirola and associates (3, 4) reported that the outer and inner cortical cells of dog kidney exhibited the specific binding to [³H]quinuclidinyl benzilate (QNB). An autoradiographic study also showed that muscarinic receptors were localized in the cortical and medullary tubules of the rat kidney (5). McArdle et al. (6) showed that carbachol (CCh) stimulated phosphoinositide hydrolysis in the rabbit medullary tubules. Although these early studies did not show exact nephron segments having ACh receptors, McArdle et al. (7) demonstrated the specific [³H]QNB binding in the rabbit inner medullary collecting duct (CD) cells. Marchetti et al. (8) reported that both CCh and ACh increased intracellular Ca^{2+} ($[\text{Ca}^{2+}]_i$) in the rat outer medullary collecting tubules. These findings indicate that muscarinic receptors exist, if not exclusively, in the CD.

Functional significance of muscarinic receptors in the CD has not been fully understood. CCh has been demonstrated to inhibit the arginine vasopressin-stimulated water flow in the rabbit cortical collecting duct (CCD) by increasing $[\text{Ca}^{2+}]_i$ (9). In the toad bladder, both ACh and CCh have been shown to inhibit Na^+ transport (10). It has been also reported that CCh inhibits NaCl absorption in ileal villus cells (11). Therefore, it is possible that ACh may also inhibit Na^+ transport in the renal tubule. However, it has never been tested whether muscarinic agonists inhibit Na^+ transport in the collecting duct. The Na^+ transport in the CCD is thought to occur through both the Na^+ channel in the apical membrane and the Na^+-K^+ ATPase in the basolateral membrane. The aim of the present study was to clarify whether ACh directly affected the Na^+ transport in the CCD. Therefore, we investigated the effect of ACh on the function of the rabbit CCD perfused in vitro using the conventional microelectrode technique and the microscopic fluorescence spectrophotometry method.

Methods

In vitro microperfusion of isolated tubules. The segments of isolated CCD were perfused in vitro according to the method of Burg et al. (12) with slight modifications as reported previously from our laboratory (13, 14). In brief, segments of the CCD were isolated from male Japa-

nese white rabbits weighing 1.5–3.0 kg. Animals were maintained on a regular rabbit laboratory diet and allowed free access to tap water. Rabbits were anesthetized with pentobarbital (35 mg/kg, i.v.) and their kidneys were removed. Then thin kidney slices were made and transferred to a cooled dish (4–6°C) containing modified Collins' solution containing (in mM): 14 KH₂PO₄, 44 K₂HPO₄, 14 KCl, 8 NaHCO₃, and 160 sucrose (pH 7.4). The CCD segment was dissected with fine forceps under a stereomicroscope.

An isolated tubule was transferred to a bath fixed on an inverted microscope (IMT-2, Olympus, Tokyo) equipped with a set of microperfusion system (Narishige, Tokyo) and perfused *in vitro* as previously described (13, 14). The tubular lumen was perfused at a rate of 10–20 nl/min by hydrostatic pressure by varying the height of the fluid reservoir which was connected to the back end of the perfusion pipette. To achieve rapid exchange of the bathing solution, the perfusion chamber was made to have a volume of 0.1 ml having a runoff groove in series. The temperature of the bathing solution was kept at 37°C by adjusting the temperature of the heating jacket. The flow rate of the bathing solution was adjusted at ~8–10 ml/min, allowing the bathing solution to be exchanged within 10 s.

Electrical measurements. The transepithelial voltage (V_T) and the voltage deflection at the proximal end of the tubule (ΔV_0) were measured through a microelectrode transmurally punctured into the tubular lumen, which was connected to one channel of a dual electrometer (Duo 773, WP Instruments, New Haven, CT). A flowing boundary 3 M KCl-agar bridge which was connected to a calomel half cell was placed at the outflow of the bath and served as a system ground. Through the perfusion pipettes current (I_0) was injected into the tubular lumen when the transepithelial resistance (R_T) and the fractional resistance of the apical membrane (fR_A) were measured. The advantage of separating current-injection and voltage-measuring channels in the perfusion pipettes has been described by other investigators (15, 16). The current (usually 50–100 nA) was injected by a stimulator (SEN-7103, Nihon Koden, Tokyo) with the other channel of electrometer (Duo773) which has a built-in stimulus isolator serving as a constant current source. Voltage deflection at the distal end of the tubule (ΔV_L) was measured by a 3 M KCl-agar bridge inserted into the collecting pipette, which was connected to a hand made high impedance voltage follower.

The transepithelial resistance was measured by finite cable analysis assuming that both terminals of the cable were closed (15, 16). The following six cable equations were used. The tubular length constant (λ) was calculated from

$$\lambda = L/\cosh^{-1}(\Delta V_0/\Delta V_L), \quad (1)$$

where ΔV_0 and ΔV_L are the voltage deflections of the proximal and the distal end of the perfused tubule, respectively. L is the cable length of the perfused tubule. The specific transepithelial resistance was measured as

$$R_T = 2\pi\lambda(\Delta V_0/I_0) \tanh(L/\lambda), \quad (2)$$

where I_0 is a current pulse injected into tubular lumen. Because the voltage deflection at the proximal end of the tubule (ΔV_0) was a linear function of the injected current over the wide range from –200 to +200 nA, we have used the current of 50–100 nA with a duration of 500 ms. The core resistance (R_C) and electrical radius (r_E) were evaluated as

$$R_C = (\Delta V_0/\lambda I_0) \tanh(L/\lambda) \quad (3)$$

$$r_E = (\rho/\pi R_C)^{1/2}, \quad (4)$$

where ρ is volume resistivity of the luminal fluid. The electrical radius was compared to the optical radius (ρ_O) as a check of the internal consistency of the cable analysis technique. Experiments with ratio of r_E/ρ_O between 0.8 and 1.2 were accepted as being reliable.

The basolateral membrane potential (V_B) was measured with conventional microelectrodes fabricated as previously (13, 14). They were filled with 0.5 M KCl solution and had resistance of 120–180 MΩ and

negligible tip potential (<5 mV). They were fixed to a microelectrode holder containing Ag/AgCl-pellet and connected to a high-impedance electrometer (model 8100, single-electrode system, Dagan, Minneapolis, MN). To impale tubular cells, a microelectrode was positioned against the basolateral membrane with a hydraulic micromanipulator (MO-102N-1, Narishige), which was mounted on another micromanipulator (MN-1, Narishige) fixed to the stage of the inverted microscope. The microelectrode was advanced into the cell by using current oscillations ("Buzz").

Fractional resistance of the apical membrane (fR_A) was calculated from

$$fR_A = 1 - \Delta V_B/\Delta V_X, \quad (5)$$

where ΔV_B is the current-induced voltage deflection of the basolateral membrane potential. The deflection of transepithelial voltage at the site of microelectrode puncture (ΔV_X) was calculated as

$$\Delta V_X = \Delta V_0 \cosh((L-X)/\lambda)/\cosh(L/\lambda), \quad (6)$$

where X is the axial distance between the mouth of the current injecting pipette and the puncture site with a microelectrode. All voltages (V_T , V_L , and V_B) were recorded on a multipen recorder (R-306, Rikadenki, Tokyo). Figures depicted in the present manuscript were digitized from original trace records through an image scanner (PC-IN506, NEC, Tokyo), and redrawn with a laser printer (Laser Jet III, Yokogawa-Hewlett-Packard, Tokyo).

Peanut agglutinin (PNA) binding study. Fluorescence of perfused tubules was observed by an inverted fluorescence microscope (OSP-3, Olympus). To identify β -intercalated (β -IC) cells, FITC-labeled PNA (10 μ g/ml) was loaded from the lumen for 5 min at 37°C (17). After loading, the tubules were excited at 490 nm and observed under high magnification. A cell with a characteristic lectin cap on the edge of the tubule was identified as a β -IC cell. To test the effect of ACh on β -IC cell, we impaled the microelectrode into the PNA-positive cell.

Intracellular Ca^{2+} concentration measurements. We measured $[\text{Ca}^{2+}]_i$ using fura 2, a fluorescent Ca^{2+} indicator, as previously reported (14, 18, 19). Isolated microperfused tubules were incubated in 200 μ l of standard bicarbonate buffer solution containing 20 μ M ace-toxymethyl ester of fura 2 (fura 2-AM, Dojin Biochemical, Kumamoto) at room temperature (22–25°C) for 20 min. Intracellular Ca^{2+} concentration ($[\text{Ca}^{2+}]_i$) was measured using a fluorescence microscope photometry system (OSP-3). Tubular cells were excited at 340 and 380 nm and emission was monitored at 510 nm. The fluorescent dye was excited alternately at 340 and 380 nm by spinning the sector mirror at a rate of 333 rpm. In this apparatus, it takes at least 10 ms to obtain one fluorescence ratio ($R = F340/F380$). One data point represented an arithmetical average of 100 fluorescence ratios for sampling time of 1 s. All the procedure were controlled by a computer (HP9000, model 332, Hewlett-Packard, Fort Collins, CO) and the data were plotted on a laser printer (HP Laser Jet III). $[\text{Ca}^{2+}]_i$ was calculated based on the formula described by Grynkiewicz et al. (20) as specified below:

$$[\text{Ca}^{2+}]_i = \frac{(R - R_{\min})F_{\max}}{(R_{\max} - R)F_{\min}} K_d, \quad (7)$$

where R_{\min} is the ratio at zero calcium in the bathing fluid and R_{\max} is the ratio at saturated calcium concentration. F_{\max} is the ratio at saturated calcium concentration. The effective dissociation constant K_d of 224 nM for the fura 2– Ca^{2+} complex was used as reported by Grynkiewicz et al. (20). Because it has been reported that K_d of fura 2 for Ca^{2+} varies in the presence of protein, absolute Ca^{2+} concentrations thus calculated might not be accurate enough. We report the concentration values to provide information on relative changes in Ca^{2+} concentration. Leakage of fura 2 from cells was <5% for 15 min and the auto-fluorescence on tubule was <10% compared to fluorescence of fura 2-AM-loaded tubules.

Solutions and drugs. The perfusate and the bathing solution were modified bicarbonate Krebs-Ringer solution (standard solution) containing (in mM): 115 NaCl, 5 KCl, 25 NaHCO₃, 0.8 Na₂HPO₄, 0.2

NaH_2PO_4 , 1.8 CaCl_2 , 1.0 MgCl_2 , 10 Na acetate, 8.3 D-glucose, 5.0 L-alanine. The Ca^{2+} -free solution was made by omitting CaCl_2 from and adding 1.0 mM EGTA to the standard solution. The 12 mM Cl^- solution was made by replacement of 110.8 mM NaCl with equimolar Na cyclamate. All the solution were continuously bubbled with 95% O_2 and 5% CO_2 to maintain the pH at 7.4. All the chemicals were purchased from respective companies listed as follows: acetylcholine from Wako Jyunyaku (Tokyo, Japan); atropine, pirenzepine, carbacol, amiloride, PMA, and phorbol-12,13-dibutyrate (PDBu) from Sigma Chemical Co (St. Louis, MO); and H-7 from Seikagaku Kogyo (Tokyo). In the experiments using PMA and PDBu which were dissolved in DMSO, the final concentration of DMSO in the bathing solution was made constant (0.1%) throughout the experiments.

Statistical analysis. All the data were expressed as means \pm SE. Statistical analyses were performed by either paired or nonpaired *t* test, when appropriate. The *P* value <0.05 was considered to be significant.

Results

When the isolated CCDs were perfused with artificial physiological solution at the rate of 10–20 nl/min, they showed electrophysiological characteristics similar to those reported previously with respect to V_T , V_B , fR_A , and R_T (21, 22). The averaged inner diameter was $25.0 \pm 0.6 \mu\text{m}$ ($n = 52$). The mean values of the tubular length and the length constant were $936.1 \pm 30.1 \mu\text{m}$ ($n = 52$) and $271.6 \pm 8.6 \mu\text{m}$ ($n = 52$), respectively.

Effect of ACh on electrical parameters in CD cell. Addition of ACh in the bath decreased lumen-negative V_T in the *in vitro*

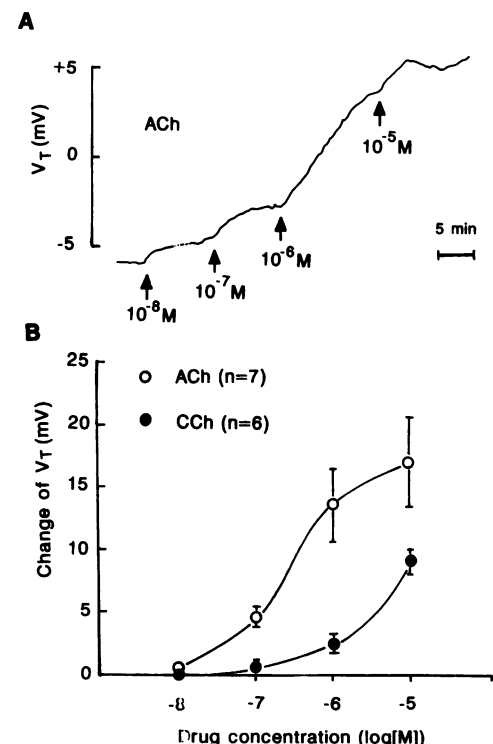


Figure 1. Effects of ACh and CCh on V_T in rabbit CCD. A representative tracing of the ACh-induced change in V_T is shown in *A*. ACh was cumulatively applied to the bathing solution. Dose-response relationships of the effects of ACh and CCh on V_T are shown in *B*. The amplitude of the agonists-induced changes of V_T are plotted against each concentration of agonists. Each points are expressed as mean \pm SE. Numbers of observations are shown in *B*.

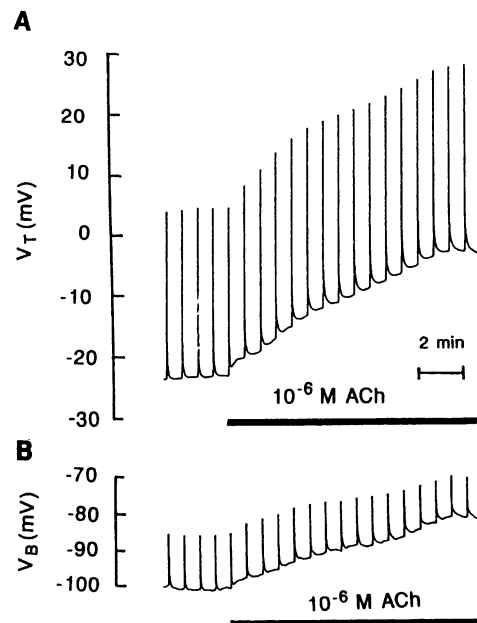


Figure 2. Representative tracings of the ACh-induced changes in electrophysiological parameters in the rabbit CCD. V_T and V_B are shown in *A* and *B*, respectively. ACh was applied in the bath during the period indicated by solid bar in each panel.

perfused rabbit CCD in a concentration-dependent manner (10^{-8} to 10^{-5} M, Fig. 1). To clarify the ionic mechanism of the ACh-induced positive deflection of V_T , we performed the cable analysis. Application of 10^{-6} M ACh to the bathing solution resulted in marked positive deflection of V_T and depolarization of V_B in the CD cell (Fig. 2, Table I). V_A significantly hyperpolarized from -70.5 ± 4.1 to -72.7 ± 3.4 mV ($n = 8$, $P < 0.05$, paired *t* test). Furthermore, both R_T and fR_A were increased by ACh (Fig. 2, Table I). These observations indicate that ACh decreases the ionic conductance of the apical membrane of the CD cell.

Effect of ACh on electrical parameters in the β -IC cell. We also examined the effect of ACh on the electrophysiological parameters in β -IC cell which was another major cell population in the rabbit CCD (22, 23). In β -IC cells, 10^{-6} M ACh applied in the bath did not change V_B and fR_A , indicating that β -IC cells do not contribute to the ACh-induced positive deflection of V_T .

Table I. Effect of ACh on Electrophysiological Parameters in Rabbit CCD

	Control	ACh	<i>n</i>	<i>P</i>
V_T (mV)	-16.9 ± 2.5	-6.7 ± 1.6	19	<0.001
R_T (Ωcm^2)	94.9 ± 7.1	111.2 ± 9.7	19	<0.001
CD cell				
V_B (mV)	-87.6 ± 4.5	-79.0 ± 3.4	8	<0.01
fR_A	0.36 ± 0.06	0.51 ± 0.06	8	<0.01
β -IC cell				
V_B (mV)	-15.9 ± 2.3	-13.4 ± 1.6	3	NS
fR_A	0.94 ± 0.01	0.95 ± 0.01	3	NS

Values are expressed as means \pm SE.

In the connecting tubule (CNT), there are two distinct types of cells: CNT and β -IC (22, 24). To ascertain that the β -IC cell does not respond to ACh, the effects of ACh on V_T and R_T were examined in the CNT. Bath application of 10^{-6} M ACh did not affect V_T (-10.0 ± 1.3 to -9.8 ± 1.3 mV; $n = 3$, NS) and R_T (16.1 ± 6.5 to 16.6 ± 6.1 Ωcm^2 ; $n = 3$, NS) in the CNT, indicating that the β -IC cell as well as the CNT cell does not participate in the ACh-induced positive deflection of V_T .

Effect of amiloride on the action of ACh. The inhibition of the apical Na^+ channel seemed to be the most plausible mechanism to account for all the ACh-induced changes of electrophysiological parameters. To confirm whether the ACh-induced responses were ascribed to the inhibition of the apical Na^+ channel, we investigated the effect of amiloride, a Na^+ channel blocker, on the action of ACh. Application of 10^{-5} M amiloride in the perfusate caused a positive deflection of V_T , a depolarization of V_B , and a hyperpolarization of V_A by 7.6 ± 3.9 mV ($P < 0.05$, $n = 4$). Both R_T and fR_A were increased by amiloride (Table II). These results confirmed that amiloride blocked the apical Na^+ conductance. In the presence of 10^{-5} M amiloride in the lumen, ACh did not change V_T , V_B , and fR_A (Table II), indicating that ACh-induced changes in electrical parameters are due to the inhibition of apical Na^+ conductance in the CCD.

Effect of ACh on intracellular calcium concentration. Bath application of ACh evoked a transient increase in $[\text{Ca}^{2+}]_i$ followed by a sustained one in a concentration-dependent fashion (10^{-8} to 10^{-5} M, Fig. 3). Concentration dependency of the action on $[\text{Ca}^{2+}]_i$ was very similar to that on V_T (Fig. 1), suggesting that the ACh-induced response is mediated by cytosolic free Ca^{2+} .

To determine the source of increased Ca^{2+} , we examined the effects of Ca^{2+} removal from either lumen or bath on the ACh-induced increase in $[\text{Ca}^{2+}]_i$. We measured the magnitude of the ACh-induced increases in $[\text{Ca}^{2+}]_i$ at the peak and 2 min after the initiation of the response that were considered to reflect a transient and a sustained component of the ACh-induced increases in $[\text{Ca}^{2+}]_i$, respectively. Ca^{2+} removal from the lumen did not alter $[\text{Ca}^{2+}]_i$. In the absence of Ca^{2+} in the luminal solution, ACh evoked a rise in $[\text{Ca}^{2+}]_i$ (peak 102.3 ± 11.9 nM, after 2 min 76.9 ± 10.2 nM; $n = 5$) to a similar extent observed in the presence of Ca^{2+} (peak 111.1 ± 11.8 nM, after 2 min 76.2 ± 9.9 nM; $n = 5$, Fig. 4). In contrast, only a small and transient increase in $[\text{Ca}^{2+}]_i$ was evoked by ACh in the absence of Ca^{2+} in the bathing solution (peak 55.0 ± 13.0 nM, after 2 min -5.6 ± 1.6 nM; $n = 6$), whereas, after repletion of Ca^{2+} to the bath, ACh evoked greater responses in a trans-

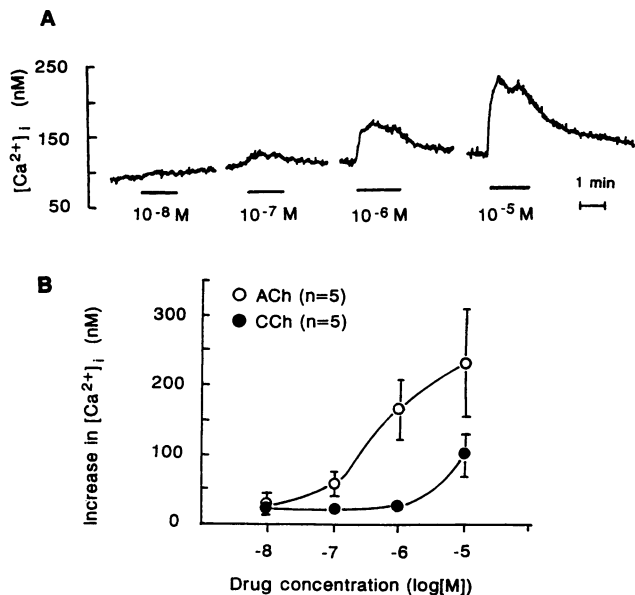


Figure 3. Effects of ACh and CCh on $[\text{Ca}^{2+}]_i$ in the rabbit CCD. Representative tracings of the ACh-induced increase in $[\text{Ca}^{2+}]_i$ are shown in A. In B, dose-response relationships of ACh and CCh for $[\text{Ca}^{2+}]_i$ are shown. Each point represents mean \pm SE. Numbers of observations are shown in B.

sient increase in $[\text{Ca}^{2+}]_i$ as well as in a sustained one (peak 83.0 ± 17.2 nM, after 2 min 51.1 ± 10.8 nM; $n = 6$, Fig. 4). These observations suggest that the ACh-induced increase in $[\text{Ca}^{2+}]_i$ occurs through two distinct pathways: a release from intracellular Ca^{2+} store site and an influx through the basolateral membrane.

Characterization of the target of ACh action. In the next series of experiments, we examined effects of muscarinic antagonists, atropine and pirenzepine, on the ACh-induced responses. In the absence of antagonists, the positive deflection of V_T to 10^{-6} M ACh was very reproducible when ACh was applied twice. The magnitude of the ACh-induced V_T changes for the first and second challenges were 7.9 ± 0.6 and 7.0 ± 0.9 mV (Fig. 5, $n = 7$, NS), respectively. Treatments by muscarinic antagonists before the second application of ACh significantly attenuated the ACh-induced responses. Atropine or pirenzepine both at 10^{-6} M decreased the ACh-induced changes of V_T from 7.8 ± 2.1 to 1.3 ± 0.7 mV ($n = 4$, $P < 0.05$) or from 11.6 ± 3.2 to 2.8 ± 1.3 mV ($n = 4$, $P < 0.05$), respectively (Fig. 5).

Both muscarinic antagonists also exhibited similar inhibitory effects on the ACh-induced increase in $[\text{Ca}^{2+}]_i$. They did not alter the baseline $[\text{Ca}^{2+}]_i$. In the presence of 10^{-6} M atropine in the bath, ACh evoked only a small rise in $[\text{Ca}^{2+}]_i$ (peak 5.2 ± 1.2 nM; $n = 5$), whereas it clearly caused a greater increase in $[\text{Ca}^{2+}]_i$ after removal of atropine (peak 66.4 ± 18.7 nM; $n = 5$, $P < 0.05$ vs. the value in the presence of atropine, Fig. 6). Although in the presence of 10^{-6} M pirenzepine in the bath, ACh produced a significant increase in $[\text{Ca}^{2+}]_i$ (peak 26.6 ± 9.1 nM; $n = 5$), in the absence of pirenzepine ACh caused much greater increase in $[\text{Ca}^{2+}]_i$ (peak 91.9 ± 30.8 nM; $n = 5$, $P < 0.05$ vs. the value in the presence of pirenzepine, Fig. 6).

Roles of calcium in the action of ACh. To ascertain whether the ACh-induced changes in electrical parameters depended on the Ca^{2+} in the peritubular fluid, we investigated the effect of

Table II. Effect of ACh on Electrophysiological Parameters in the Presence of Amiloride in the Lumen in Rabbit CCD

	Control	Amiloride	Amiloride + ACh
V_T (mV)	-17.1 ± 3.0 (6)	3.3 ± 0.8 (6)*	3.6 ± 1.0 (6)
V_B (mV)	-88.4 ± 5.1 (4)	-73.6 ± 3.3 (4)*	-70.5 ± 5.1 (4)
R_T (Ωcm^2)	77.3 ± 3.3 (6)	82.9 ± 2.7 (6)*	91.6 ± 5.1 (6)*
fR_A	0.26 ± 0.06 (4)	0.44 ± 0.08 (4)*	0.57 ± 0.13 (4)

Concentrations of amiloride and ACh were 10^{-5} and 10^{-6} M respectively. Values are expressed as means \pm SE. They were compared with the control using the paired *t*-test. * $P < 0.05$; * $P < 0.001$.

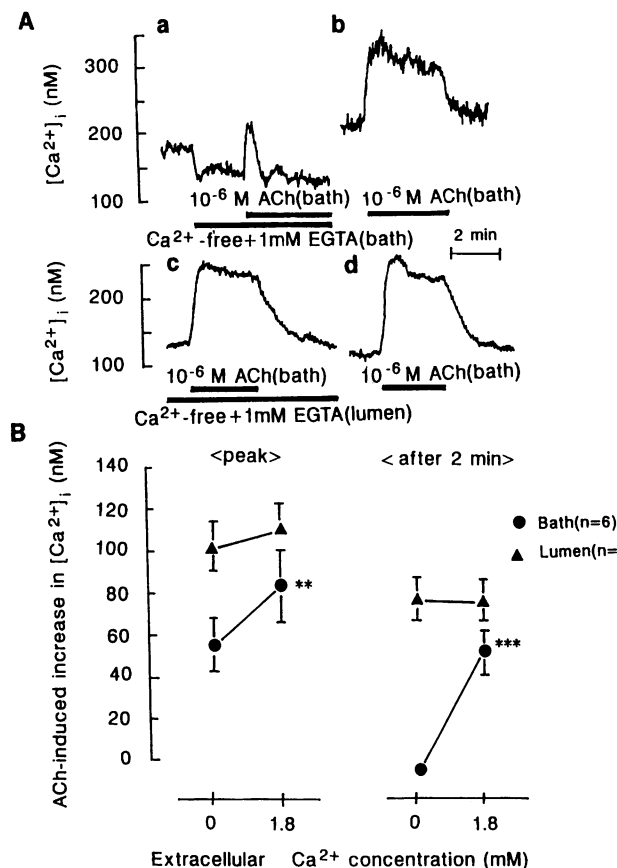


Figure 4. Effect of Ca^{2+} -removal from bath or lumen on the ACh-induced increase in $[\text{Ca}^{2+}]_i$. Representative tracings are shown in *A*. Bath application of 10^{-6} M ACh was repeated in the same tubule for two times. First and second responses were observed in the absence and presence of Ca^{2+} , respectively. Ca^{2+} was removed either from the bath or from the lumen. Periods of removal of Ca^{2+} and application of ACh are shown by solid bars in *A*. Note that Ca^{2+} removal from the bath decreased basal $[\text{Ca}^{2+}]_i$ and inhibited the sustained increase in $[\text{Ca}^{2+}]_i$ in the presence of ACh. Summarized data are shown in *B*. The amplitude of the ACh-induced increase in $[\text{Ca}^{2+}]_i$ at peak and 2 min after the initiation of the response were measured. Each point represents mean \pm SE. Numbers of observations are indicated in panel *B*. ** $P < 0.01$; *** $P < 0.005$.

ACh on V_T and R_T in the absence of Ca^{2+} in the bath ($0 \text{ mM Ca}^{2+} + 1 \text{ mM EGTA}$). Because we could not maintain the stable impalement of microelectrode in the CD cell in the Ca^{2+} -free condition, we monitored only V_T and R_T . Removal of Ca^{2+} from the bathing solution did not alter both V_T (from -11.8 ± 1.0 to -11.5 ± 1.0 mV; $n = 7$, NS) and R_T (from 84.8 ± 6.9 to $83.1 \pm 6.5 \Omega \text{cm}^2$; $n = 7$, NS). As shown in Fig. 7, only a small change of V_T (from -11.5 ± 1.0 to -8.7 ± 1.4 mV; $n = 7$, $P < 0.05$) and a tendency to increase R_T (from 83.1 ± 6.5 to $86.2 \pm 8.9 \Omega \text{cm}^2$; $n = 7$, NS) were observed by 10^{-6} M ACh in the absence of Ca^{2+} in the bath. Compared with the control group shown in Table I, removal of Ca^{2+} from the bathing solution significantly reduced the ACh-induced responses (Fig. 7), indicating that ACh requires Ca^{2+} influx through the basolateral membrane to fully evoke the changes in electrophysiological parameters in the CCD.

Effects of modulators of protein kinase C (PKC) on the action of ACh. It has been shown that phorbol esters, activators of PKC, applied in the bath reduced lumen-negative V_T and

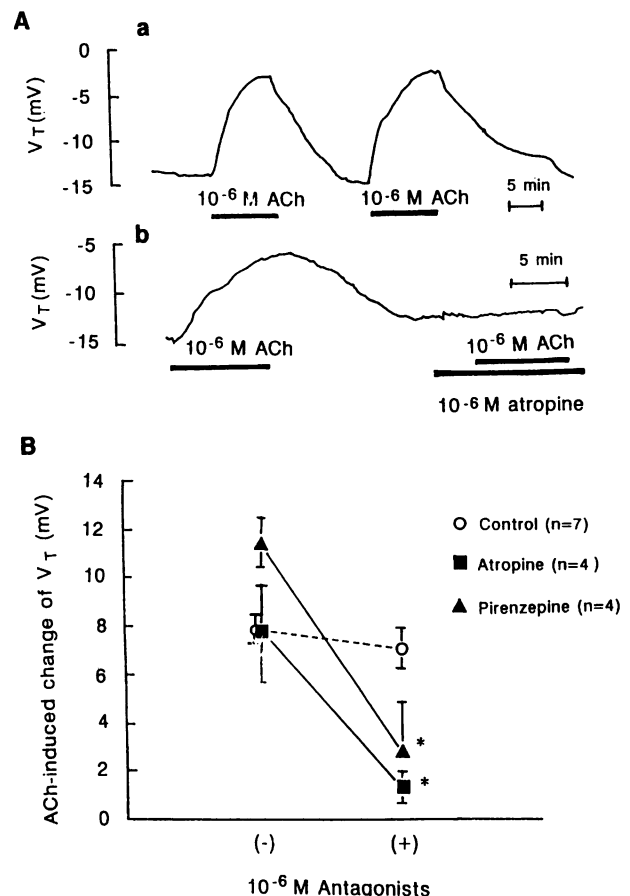


Figure 5. Effect of muscarinic receptor antagonists on the ACh-induced negative deflection of V_T in the rabbit CCD. Representative tracings are shown in *A*. Bath application of 10^{-6} M ACh was repeated twice in the same tubule. In second challenge, ACh was applied in the absence (−) or presence (+) of 10^{-6} M atropine in the bath. Drugs were applied during the period indicated by solid bars. Summarized data are shown in *B*. Each point represents mean \pm SE. Numbers of observations are shown in *B*. * $P < 0.05$.

inhibited Na^+ reabsorption in the rabbit CCD (25). It has been also reported that PGE_2 inhibits the apical Na^+ channel via the PKC pathway (26). Therefore, we tested the effects of phorbol esters, PMA and PDBu (Fig. 8), and H-7, an inhibitor of PKC (Fig. 9), on the ACh-induced responses.

Either PMA or PDBu added in the bath at the concentration of 10^{-7} M shifted V_T from -11.5 ± 2.2 to -4.0 ± 1.0 mV ($n = 7$, $P < 0.01$) and from -14.3 ± 1.3 to -6.0 ± 1.2 mV ($n = 4$, $P < 0.005$) and increased R_T from 79.1 ± 5.4 to $85.5 \pm 4.7 \Omega \text{cm}^2$ ($n = 7$, $P < 0.05$) and from 74.4 ± 6.0 to $84.1 \pm 6.8 \Omega \text{cm}^2$ ($n = 4$, $P < 0.05$), respectively (Fig. 8). These actions of phorbol esters were completely attenuated by luminal application of 10^{-5} M amiloride. In the presence of amiloride in the lumen, PMA did not change V_T (from 2.2 ± 0.9 to 1.4 ± 0.6 mV; $n = 5$, NS) or R_T (from 86.9 ± 7.2 to $91.9 \pm 8.9 \Omega \text{cm}^2$; $n = 5$, NS). Under the same condition, PDBu did not alter V_T (from 1.0 ± 0.4 to 0.9 ± 0.5 mV, $n = 4$, NS) or R_T (from 73.8 ± 11.2 to $75.3 \pm 11.2 \Omega \text{cm}^2$; $n = 4$, NS) as well. These observations confirmed that the responses induced by PMA or PDBu were mainly due to inhibition of the apical Na^+ channel. After the treatment with 10^{-7} M PMA for 10–15 min, 10^{-6} M ACh produced only a slight change in V_T (from -4.0 ± 1.0 to -3.0 ± 1.0 mV; $n = 7$, P

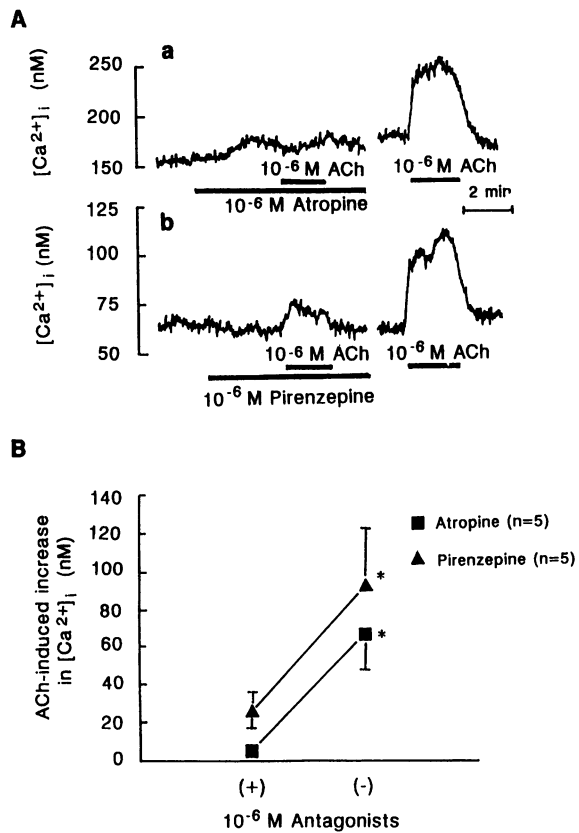


Figure 6. Effects of muscarinic receptor antagonists on the ACh-induced increase in $[Ca^{2+}]_i$. Typical tracings are shown in A. ACh at 10⁻⁶ M was applied in the bath in the same tubule for two times. First and second responses were observed in the presence (+) and absence (-) of antagonist, respectively. Drugs were applied during the period indicated by solid bars. Summarized data are shown in B. Each point represents mean \pm SE. Numbers of observations are shown in B. * $P < 0.05$.

< 0.05) and no change in R_T (from 85.5 \pm 4.7 to 87.1 \pm 5.3 Ωcm^2 ; $n = 7$, NS). Exposure to 10⁻⁷ M PDBu from the bath also masked the ACh-induced responses (V_T from -6.0 ± 1.2 to -5.3 ± 0.9 mV, $n = 4$, NS; R_T from 84.1 \pm 6.8 to 89.7 \pm 8.1 Ωcm^2 , $n = 4$, NS).

Bath application of H-7 (3 \times 10⁻⁵ M) did not cause any changes of V_T (from -14.7 ± 3.4 to -15.5 ± 3.0 mV; $n = 4$, NS) and R_T (from 87.5 \pm 16.6 to 86.2 \pm 15.4 Ωcm^2 , $n = 4$, NS). In the presence of H-7 in the bath, addition of 10⁻⁶ M ACh showed a tendency to decrease lumen-negative V_T (from -15.5 ± 3.0 to -10.5 ± 2.6 mV; $n = 4$, NS) and a significant increase in R_T (from 86.2 \pm 15.4 to 92.0 \pm 16.0 Ωcm^2 ; $n = 4$, $P < 0.05$). Compared with the control group (shown in Table I), however, the action of 10⁻⁶ M ACh was apparently reduced by H-7 (Fig. 9).

Discussion

We reported here that ACh inhibited the amiloride-sensitive apical Na^+ conductance in the CD cell of the rabbit CCD by an activation of muscarinic receptor located in the basolateral membrane and that the ACh-induced responses were mediated by the combination of an increase in $[Ca^{2+}]_i$ and a PKC activation.

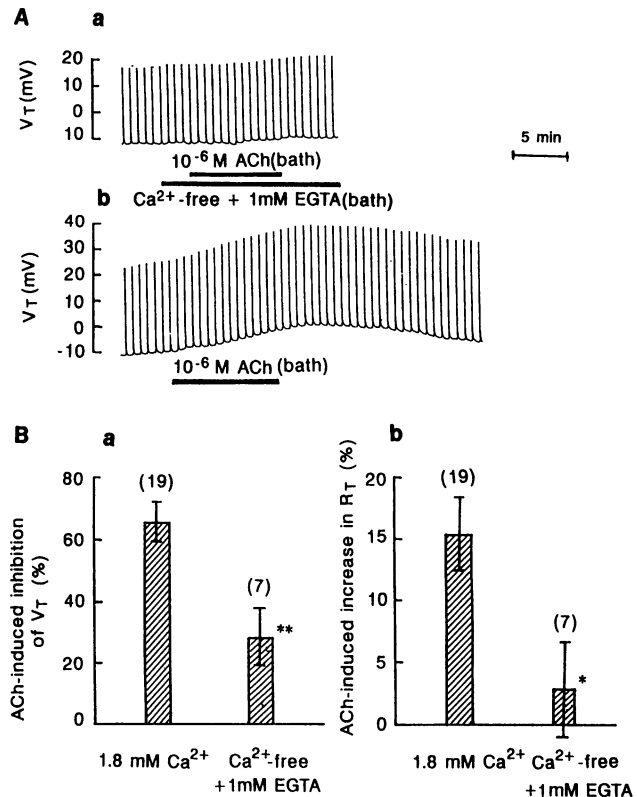


Figure 7. Effect of Ca^{2+} -removal from bath on the ACh-induced changes of V_T and R_T . Representative tracings are shown in A. Periods of removal of Ca^{2+} and application of ACh are shown by solid bars. The recordings shown in Aa and Ab were obtained from different tubules. Summarized data are shown in B. The ACh-induced inhibition of lumen-negative V_T (Ba) and the ACh-induced increase in R_T (Bb) are compared between the conditions in the presence and absence of Ca^{2+} in the bath. The data are expressed as mean \pm SE. Numbers of observations are indicated on the top of each column. * $P < 0.05$; ** $P < 0.01$, compared to the control values.

Target cell of ACh in the rabbit CCD. Three distinct types of cells (CD, α -IC, and β -IC cells) can be identified in the rabbit CCD by the conventional microelectrode method (22). The CD cells possess a relatively high V_B and a low fR_A , whereas IC cells have a relatively low V_B and a high fR_A which is close to unity. Although IC-cells have high Cl^- conductance in the basolateral membrane, α -IC cells are distinct from β -IC cells in that they lack Cl^- entry steps in the apical membrane. Because IC-cells in the early portion of the rabbit CCD are mainly β -IC cells (22, 23), we did not test the effect of ACh on the α -IC cell in the present study. We identified the β -IC cell by the following criteria: (a) the apical membrane is stained by FITC-peanut lectin; (b) the resting V_B is shallow, being less than -30 mV; and (c) a reduction of luminal Cl^- concentration causes marked hyperpolarization of the V_B . ACh greatly affected the electrophysiological parameters in the CD cells, but not in the β -IC cells (Table I). The β -IC cells are also found in the CNT and are distinguishable from the CNT cells electrophysiologically (22, 23). Bath application of ACh did not change V_T and R_T in the CNT. Taken together, we conclude that ACh has no effect on the ionic conductance of the β -IC cells and that the target cell of ACh is the CD cells in the rabbit CCD.

ACh inhibits the apical Na^+ channel in the CD cell. In the present study, we demonstrated that ACh caused a positive V_T

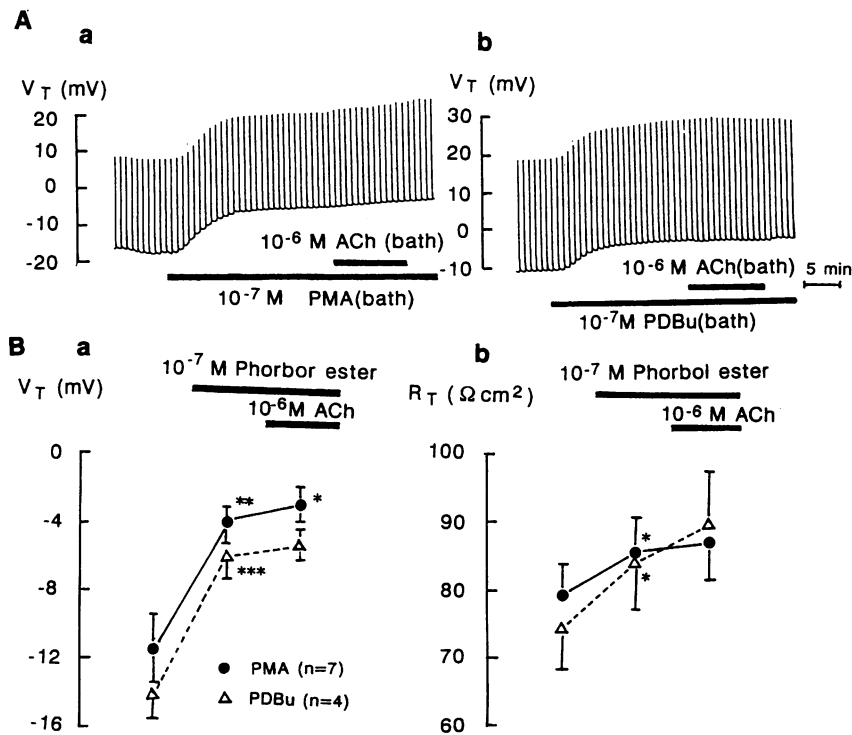


Figure 8. Effects of phorbol esters on V_T and R_T in the rabbit CCD. Representative tracings are shown in A. Note that, in the presence of either PMA (Aa) or PDBu (Ab), ACh did not produce any additional effects. Phorbol esters and ACh were added in the bath during the period indicated by solid bars in this figure. Summarized data are shown in B. The data are expressed as mean \pm SE. Numbers of observations are shown in B. * $P < 0.05$; ** $P < 0.01$; *** $P < 0.005$, compared to the left values.

deflection and an increase in R_T . These effects were closely associated with the actions of ACh in hyperpolarizing the apical membrane and increasing fR_A of the CD cell. These findings are best explained by the hypothesis that ACh inhibits Na^+

channel in the apical membrane. This hypothesis is further strengthened by the observation that effects of ACh were not observed in the presence of amiloride which blocks Na^+ channel in the apical membrane.

If a Cl^- channel exists in the apical membrane in the CD cell, its inhibition will lead to similar changes of electrophysiological parameters induced by ACh. At the present, there are no evidences which prove the existence of Cl^- channel in the apical membrane of the CD cell. Sansom et al. (27) provided evidence for the absence of a significant Cl^- conductance in the apical membrane of the CD cell. Therefore, it is unlikely that the inhibition of the apical Cl^- channel accounts for the ACh-induced responses.

Although the CD cell has a high K^+ conductance in the apical membrane (21), it is unlikely that the increase in fR_A by ACh is due to an inhibition of the K^+ conductance. If ACh inhibited the apical K^+ conductance, the apical membrane would be depolarized rather than hyperpolarized and V_T would be deflected to a more negative level.

Muscarinic receptor is involved in the ACh-induced responses. Several investigators have provided the evidence for the existence of muscarinic receptors in the tubular cells. According to their data, muscarinic receptors were mainly present in the collecting duct cells and were more abundant in the medulla than in the cortex (5, 7). However, little information is available about the characteristics of the receptor type in detail. ACh applied in the bath produced a positive deflection of V_T and an increase in $[Ca^{2+}]_i$. These effects of ACh were antagonized by both atropine and pirenzepine. The antagonistic effect of atropine was tended to be more potent than that of pirenzepine (Figs. 5 and 6). Although CCh also evoked the responses similar to those of ACh, the potency was $<10\%$ that of ACh. Our results were compatible with the view of Marchetti et al. (8) deduced from the observations of $[Ca^{2+}]_i$ in the rat outer medullary CD. The M_1 and M_3 types of muscarinic ACh

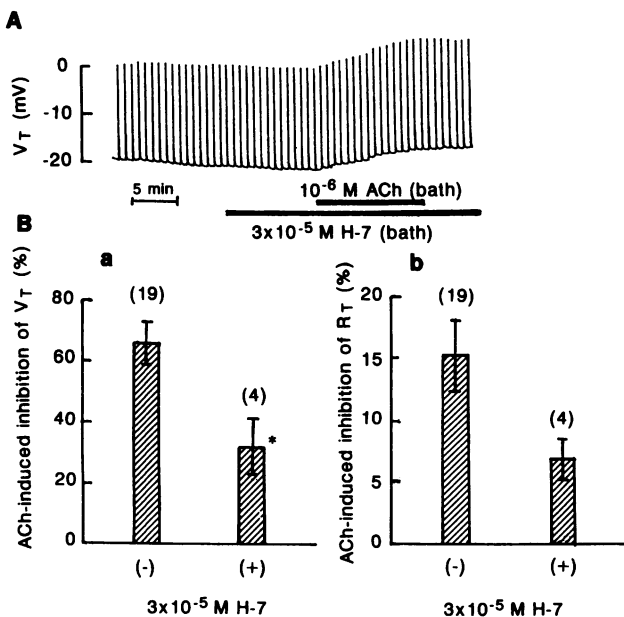


Figure 9. Effect of H-7 on the ACh-induced changes of V_T and R_T . Representative tracings are shown in A. Summarized data are shown in B. ACh and H-7 were applied to the bathing solution during the period indicated by solid bars in this figure. The ACh-induced inhibition of lumen-negative V_T (Ba) and the ACh-induced increase in R_T (Bb) were compared between the values in the absence and presence of H-7 in the bath, respectively. Each column represents mean \pm SE. Numbers of observations are shown on the top each column. * $P < 0.05$, compared to the control values.

receptors have been shown to couple strongly to phosphatidylinositol turnover. A M₁ receptor has been demonstrated to be highly sensitive to pirenzepine (28, 29). Taken together, it is likely that the muscarinic receptor present in the basolateral membrane in rabbit CD cell is of the M₁ type. However, further investigations are required to determine the exact type of receptor.

Role of intracellular Ca²⁺. A number of experiments have demonstrated that an increase in [Ca²⁺]_i inhibits the Na⁺ transport in tight epithelia, such as urinary bladder and ileum (11, 10). Agents which increase [Ca²⁺]_i, such as PGE₂ (27, 30, 31), EGF (32–34) and ionomycin (35), were also reported to inhibit the Na⁺ transport in the CCD. In the present study, ACh applied in the bath evoked a sustained increase in [Ca²⁺]_i and inhibited the apical Na⁺ channel. Both the concentration-response relationships of V_T and [Ca²⁺]_i in response to ACh were quite similar. The removal of Ca²⁺ from the bath, but not from the lumen, partially attenuated the peak amplitude of the ACh-induced rise of [Ca²⁺]_i and did completely abolish the sustained component, indicating that ACh increases [Ca²⁺]_i via both a release from intracellular store site and an influx across the basolateral membrane. The most parts of the ACh-induced changes of electrophysiological parameters were also attenuated by omission of Ca²⁺ from the bathing solution, suggesting that for the action of ACh the Ca²⁺ influx across the basolateral membrane is required. We could not determine whether intracellular free Ca²⁺ directly or indirectly inhibited the apical Na⁺ channel. Palmer and Frindt (36) reported that cytoplasmic Ca²⁺ had no effect on Na⁺ channel in inside-out membrane patch of the rat CCD. Therefore, it is possible that cytoplasmic Ca²⁺ ion indirectly inhibits Na⁺ channel via activation of other signal transduction pathways.

Removal of Ca²⁺ from the bath, but not from the lumen, caused a significant fall in basal [Ca²⁺]_i and a marked attenuation of the ACh-induced sustained increase in [Ca²⁺]_i, strongly indicating that Ca²⁺ permeable pathway exists in the basolateral membrane. Evidence which suggests the existence of Ca²⁺ entry pathway in the basolateral membrane of the rat CCD has been also demonstrated (37). Recently, we have demonstrated that the application in the bath of manidipine, a dihydropyridine-type of Ca²⁺ channel blocker, decreases basal [Ca²⁺]_i and attenuated the agonist-induced sustained increase in [Ca²⁺]_i in the CD cell of the rabbit CCD (18). This would strongly suggest that the dihydropyridine-sensitive Ca²⁺ channel is present in the basolateral membrane of the CD cell and plays roles in the regulation of both basal [Ca²⁺]_i and the agonist-induced increase in [Ca²⁺]_i. Therefore, it is possible that ACh evokes a sustained increase in [Ca²⁺]_i by the enhancement of Ca²⁺ influx through the dihydropyridine-sensitive Ca²⁺ channel in the basolateral membrane. Marchetti et al. (8) reported that 10 μM nifedipine failed to block the increase in [Ca²⁺]_i caused by CCh and argued that the Ca²⁺ entry mechanism across the basolateral membrane of the CCD may be distinct from dihydropyridine sensitive Ca²⁺ channel. Because we did not examined the effect of dihydropyridine in this particular study, the exact nature of the basolateral Ca²⁺ entry must await further investigations.

Role of PKC. It has been demonstrated that PGE₂ inhibits Na⁺ channel via an activation of PKC (24). Hays et al. (25) reported that phorbol esters inhibits Na⁺ reabsorption and decreases lumen-negative V_T. Activators of PKC (PMA and 1-oleyl-2-acetyl glycerol) have been shown to inhibit single Na⁺

channel in A6 amphibian distal nephron cell line (38, 39). In the Ca²⁺-free condition in the bath in our study, ACh evoked only a transient increase in [Ca²⁺]_i, indicating that ACh stimulates the production of IP₃ which releases Ca²⁺ from the internal store site (6). It is possible that an increase in IP₃ production is accompanied in parallel by an increase in diacylglycerol, an endogenous activator of PKC (40). Therefore, we assumed that ACh inhibited the apical Na⁺ channel by an activation of PKC. Such assumption is supported by our following findings: (a) both PMA and PD₈₁ inhibited the apical Na⁺ channel; (b) in the presence of either PMA or PD₈₁, ACh produced little or no additional changes of electrophysiological parameters; and (c) H-7 partially attenuated the ACh-induced responses. These results strongly suggest that the activation of PKC in part contributed to the ACh-induced inhibition of the apical Na⁺ channel in the rabbit CCD.

Physiological significance of the ACh-induced inhibition of the apical Na⁺ channel in the CCD. Infusion of ACh into the renal artery have been demonstrated to increase in renal plasma flow, urine volume, and Na⁺ excretion without affecting GFR in dogs (1, 2). Both actions of ACh on renal vessels and on tubular reabsorption may account for such phenomena. It has been suggested that the renal actions of ACh were partially mediated by prostaglandins (2). Although other mediators might contribute to the ACh-induced natriuresis, our results strongly suggest that ACh causes natriuresis via an inhibition of Na⁺ reabsorption across the CD cells of the CCD.

Acknowledgments

We express our thanks to Ms. Keiko Sakai for secretary work and Ms. Yuki Oyama for technical assistance in the processes of this study.

This study was supported in part by a grant from Salt Science Foundation (No. 92037).

References

1. Vander, A. J. 1964. Effects of acetylcholine, atropine, and physostigmine on renal function in the dog. *Am. J. Physiol.* 206:492–498.
2. Yun, J. C. H., G. Oriji, J. R. Gill Jr., B. R. Coleman, J. Peters, and H. Keiser. 1993. Role of muscarinic receptors in renal response to acetylcholine. *Am. J. Physiol.* 265:F46–F52.
3. Pirola, C. J., A. L. Alvarez, M. S. Balda, S. Finkelman, and V. E. Nahmod. 1989. Evidence for cholinergic innervation in dog renal tissue. *Am. J. Physiol.* 257:F746–F754.
4. Pirola, C. J., A. L. Alvarez, S. Finkelman, and V. E. Nahmod. 1991. Release of acetylcholine from isolated canine renal tissue. *Am. J. Physiol.* 260:F198–F203.
5. De Michele, M., F. Amenta, and C. Cavallotti. 1989. Autoradiographic localization of muscarinic receptors within the rat kidney. *Eur. J. Pharmacol.* 169:297–305.
6. McArdle, S., L. C. Garg, and F. T. Crews. 1988. Cholinergic stimulation of phosphoinositide hydrolysis in rabbit kidney. *J. Pharmacol. Exp. Ther.* 244:586–591.
7. McArdle, S., L. C. Garg, and F. T. Crews. 1989. Cholinergic receptors in renal medullary collecting duct cells. *J. Pharmacol. Exp. Ther.* 248:12–16.
8. Marchetti, J., S. Taniguchi, F. Lebrun, and F. Morel. 1990. Cholinergic agonists increase cell calcium in rat medullary collecting tubules: a fura-2 study. *Pflügers Arch. Eur. J. Physiol.* 416:561–567.
9. Snyder, H. M., D. M. Fredin, and M. D. Breyer. 1991. Muscarinic receptor activation inhibits AVP-induced water flow in rabbit cortical collecting ducts. *Am. J. Physiol.* 260:F929–F936.
10. Wiesmann, W., S. Sinha, J. Yates, and S. Klahr. 1978. Cholinergic agents inhibit sodium transport across the isolated toad bladder. *Am. J. Physiol.* 235:F564–F569.
11. Cohen, M. E., J. Wesolek, J. McCullen, K. Rys-Sikora, S. Pandol, R. P. Rood, G. W. G. Sharp, and M. Donowitz. 1991. Carbachol- and elevated Ca²⁺-induced translocation of functionally active protein kinase C to the brush border of rabbit ileal Na⁺ absorbing cells. *J. Clin. Invest.* 88:855–863.

12. Burg, M., J. Grantham, M. Abramow, and J. Orloff. 1966. Preparation and study of fragments of single rabbit nephrons. *Am. J. Physiol.* 210:1293-1298.

13. Yoshitomi, K., C. Koseki, J. Taniguchi, and M. Imai. 1987. Functional heterogeneity in the hamster medullary thick ascending limb of Henle's loop. *Pflügers Arch. Eur. J. Physiol.* 408:600-608.

14. Takeda, M., K. Yoshitomi, and M. Imai. 1993. Endogenous adenosine stimulates basolateral Na^+ - HCO_3^- cotransporter in rabbit proximal convoluted tubule. *Am. J. Physiol.* 265:F511-F519.

15. Beyenbach, K. W., and E. Frömter. 1985. Electrophysiological evidence for Cl secretion in shark renal proximal tubules. *Am. J. Physiol.* 248:F282-F295.

16. Sackin, H., and E. L. Boulpaep. 1981. Isolated perfused salamander proximal tubule: methods, electrophysiology, and transport. *Am. J. Physiol.* 241:F39-F52.

17. Hayashi, M., Y. Yamaji, M. Iyori, W. Kitajima, and T. Saruta. 1991. Effect of isoproterenol on intracellular pH of the intercalated cells in the rabbit cortical collecting ducts. *J. Clin. Invest.* 87:1153-1157.

18. Kurokawa, K., K. Yoshitomi, M. Ikeda, S. Uchida, M. Naruse, and M. Imai. 1993. Regulation of cortical collecting duct function: effect of endothelin. *Am. Heart J.* 125:582-588.

19. Shimizu, T., M. Naruse, M. Takeda, M. Nakamura, K. Yoshitomi, and M. Imai. 1992. Mechanism of PGE_2 -induced cell swelling in distal nephron segments. *Am. J. Physiol.* 263:F824-F832.

20. Grynkiewicz, G., M. Poenie, and R. Y. Tsien. 1985. A new generation of Ca^{2+} indicators with greatly improved fluorescence properties. *J. Biol. Chem.* 260:3440-3450.

21. Koeppen, B. M., B. A. Biagi, and G. H. Giebisch. 1983. Intracellular microelectrode characterization of the rabbit cortical collecting duct. *Am. J. Physiol.* 244:F35-F47.

22. Muto, S., K. Yasoshima, K. Yoshitomi, and M. Imai, Y. Asano. 1990. Electrophysiological identification of α - and β -intercalated cells and their distribution along the rabbit distal nephron segments. *J. Clin. Invest.* 86:1829-1839.

23. Schwartz, G. J., J. Barasch, and Q. Al-Awqati. 1985. Plasticity of functional epithelial polarity. *Nature (Lond.)*. 318:368-371.

24. Yoshitomi, K., T. Shimizu, and M. Imai. 1988. Functional cellular heterogeneity in the rabbit connecting tubule. *Kidney Int.* 33:430. (Abstr.)

25. Hays, S. R., M. Baum, and J. P. Kokko. 1987. Effects of protein kinase C activation on sodium, chloride, and total CO_2 transport in the rabbit cortical collecting tubule. *J. Clin. Invest.* 80:1561-1570.

26. Ling, B. N., K. E. Kokko, and D. C. Eaton. 1992. Inhibition of apical Na^+ channels in rabbit cortical collecting tubules by basolateral prostaglandin E_2 is modulated by protein kinase C. *J. Clin. Invest.* 90:1328-1334.

27. Sansom, S. C., E. J. Weinman, and R. G. O'Neil. 1984. Microelectrode assessment of chloride-conductive properties of cortical collecting duct. *Am. J. Physiol.* 247:F291-F302.

28. Goyal, R. K. 1989. Muscarinic receptor subtypes: physiology and clinical implications. *N. Engl. J. Med.* 321:1022-1029.

29. Lechleiter, J., E. Peralta, and D. Clapham. 1989. Diverse functions of muscarinic acetylcholine receptor subtypes. *Trends Pharmacol. Sci.* 10 (Suppl. IV):34-38.

30. Hébert, R. L., H. R. Jacobson, and M. D. Breyer. 1991. Prostaglandin E_2 inhibits sodium transport in rabbit cortical collecting duct by increasing intracellular calcium. *J. Clin. Invest.* 87:1992-1998.

31. Iino, Y., and M. Imai. 1978. Effects of prostaglandins on Na transport in isolated collecting tubules. *Pflügers Arch. Eur. J. Physiol.* 373:125-132.

32. Muto, S., H. Furuya, K. Tabei, and Y. Asano. 1991. Site and mechanism of action of epidermal growth factor in rabbit cortical collecting duct. *Am. J. Physiol.* 260:F163-F169.

33. Vehaskari, V. M., J. Herndon, and L. L. Hamm. 1991. Mechanism of sodium transport inhibition by epidermal growth factor in cortical collecting ducts. *Am. J. Physiol.* 261:F896-F903.

34. Warden, D. H., and J. B. Stokes. 1993. EGF and PGE_2 inhibit rabbit CCD Na^+ transport by different mechanisms: PGE_2 inhibits Na^+ - K^+ pump. *Am. J. Physiol.* 264:F670-F67735.

35. Frindt, G., and E. E. Windhager. 1990. Ca^{2+} -dependent inhibition of sodium transport in rabbit cortical collecting tubules. *Am. J. Physiol.* 258:F568-F582.

36. Palmer, L. G., and G. Frindt. 1987. Ca ionophore and phorbol ester inhibit Na channels in rat cortical collecting tubules. *Fed. Proc.* 46:495. (Abstr.)

37. Taniguchi, S., J. Marchetti, and F. Morel. 1989. Cytosolic free calcium in single microdissected rat cortical collecting tubules. *Pflügers Arch. Eur. J. Physiol.* 414:125-133.

38. Ling, B. N., and D. C. Eaton. 1989. Effects of luminal Na^+ on single Na^+ channels in A6 cells, a regulatory role for protein kinase C. *Am. J. Physiol.* 256:F1094-F1103.

39. Yanase, M., and J. S. Handler. 1986. Activators of protein kinase C inhibit sodium transport in A6 epithelia. *Am. J. Physiol.* 250:C517-C522.

40. Nishizuka, Y. 1988. The molecular heterogeneity of protein kinase C and its implications for cellular regulation. *Nature (Lond.)*. 334:661-665.